Construction and Building Materials 388 (2023) 131683

Contents lists available at ScienceDirect

Construction and Building Materials

journal homepage: www.elsevier.com/locate/conbuildmat

Lateral pressure of nano-engineered SCC combining nanoclays, nanosilica and viscosity modifying admixtures

Hugo Varela, Gonzalo Barluenga [*], Javier Puentes, Irene Palomar, Angel Rodriguez

Department of Architecture, Universidad de Alcala, Madrid, Spain

A R T I C L E I N F O

Keywords:
Lateral pressure
SCC
Nanoclays
Nanosilica
Viscosity modifying admixtures
Capillary pressure
Structural build-up

A B S T R A C T

Self-compacting concrete (SCC) is an energy efficient building technology widely used for multiple constructive applications. However, the large flowability of fresh SCC produces an increase of the lateral pressure exerted on the formwork regarding to conventional concretes. One solution to reduce the maximum lateral pressure (P_{max}) is to modulate the fresh performance of SCC by the addition of rheology modifiers. Among them, nanocomponents highlight due to their larger efficiency derived from their tiny particle size. In this study, the efficiency of nano-engineered SCC (NE-SCC) combining small amounts of nanocomponents, as nanoclays and nanosilica, with viscosity modifying admixtures (VMAs) to decrease P_{max} is explored. Lateral pressure exerted by NE-SCC on cylindrical columns subjected to self-weight and to air pressure was assessed using wall and capillary pressure sensors over time. It was found that the incorporation of attapulgite and bentonite nanoclays combined with VMAs could reduce P_{max}. This reduction was measured with wall and capillary pressure sensors on self-weight column and air pressure column laboratory tests, and good correlation between them over time was obtained. A predictive model of the maximum lateral Pressure (P_{max}) and its evolution over time (P_L) was proposed, related to SCC paste thixotropy ($A_{thix,p}$), casting height (H) and SCC pressure decay coefficient (C_d).

1. Introduction

Self-Compacting Concrete (SCC) is an efficient technology that helps to increase sustainability in construction. However, fresh SCC exerts larger lateral pressure (P_L) on the formwork than conventional concretes, due to its larger proportion of paste and, consequently, larger amount of water by concrete volume [1]. Due to its large flowability and low initial shear yield stress (τ_0), SCC behaves similar to a thick liquid and the Maximum lateral pressure (P_{max}) could be expected to be close to hydrostatic pressure [2]. However, many studies have measured lower values of P_{max} and some predictive models have been proposed and evaluated [3–14].

This reduction of P_{max} is a consequence of several reasons, such as friction against the formwork, compressibility of SCC due to entrained air and thixotropic effects due to flocculation [6]. SCC friction with the formwork is limited due to the low yield stress of SCC and its increase would reduce self-compactability. The same happens with the entrained air, which should not be too large if an adequate mechanical performance is required. Accordingly, the most feasible way to reduce P_{max} is to increase SCC thixotropy [6,11,15].

Thixotropy can be defined as the increase of shear yield stress over time of mixtures left at rest (structural build-up at rest) and is produced by a combination of reversible and irreversible mechanisms [2,16–23]. Reversible mechanisms are related to bonding forces that can be broken if subjected to shear forces and can be described by a thixotropy coefficient (A_{thix}), while irreversible mechanisms correspond to the structuration of the mixture due to cement hydration and percolation [23].

SCC thixotropy can be enhanced incorporating inorganic additions and organic admixtures commonly known as rheology modifiers. Among inorganic additions, nano components (NC) as nano-silica and nano-clays have been used as rheology modifiers for nano-engineered SCC due to the large efficiency produced by their tiny particle size [24–30]. Viscosity modifying admixtures (VMAs) have also been used alone [31–34] or combined with NC to increase thixotropy, showing significant synergetic effects [15,23,35].

To analyze the effect of rheology modifiers on P_{max} exerted by SCC, different approaches have been described. One approach focused on SCC paste or mortar rheology, considering that the structural build up

* Corresponding author at: Departamento de Arquitectura, Escuela de Arquitectura, Universidad de Alcalá, C. Santa Úrsula, 8, Alcalá de Henares, 28801 Madrid, Spain.

E-mail address: gonzalo.barluenga@uah.es (G. Barluenga).

https://doi.org/10.1016/j.conbuildmat.2023.131683
Received 15 March 2023; Received in revised form 21 April 2023; Accepted 4 May 2023
Available online 10 May 2023

(thixotropy) measured on paste ($A_{thix,p}$) would produce practical effects on a multiphase mixture as SCC [5,20,23]. This scientific strategy can produce precise measurements although uncertain to be transferred to a practical scale [36]. The other approach focused on SCC samples evaluated through field-oriented rheology tests, laboratory simulations of self-weight and air pressure tests and real scale tests [1]. In general, the larger and more realistic the test, the more expensive and less repeatable [9,10,12]. The influence of measurement device types and locations in the test setup have also shown many differences in the experimental results [3–5,12].

In this study, the effect of nano-engineered SCC, mixing inorganic and organic rheology modifiers, on P_{max} exerted on laboratory column pressure tests on samples under self-weight and air pressure were assessed. Combinations of NC and VMAs were selected among those that showed higher paste thixotropy values in a previous study carried out on nano-engineered SCC paste samples [23]. The aim of the study was to evaluate the possibility of scaling the advantageous results from paste phase to obtain a nano-engineered SCC which exerts lower lateral pressure on the formwork. Also, to study wall and capillary pressure results correlation of SCC samples and to propose a predictive model to estimate the maximum lateral Pressure (P_{max}) and its evolution over time (P_L). Besides, wall and capillary pressure measurement devices and samples subjected to their own weight and to air pressure were also assessed.

2. Experimental program:

2.1. Materials and mix design

Table 1 summarizes the nano-engineered self-compacting concrete (NE-SCC) compositions designed for the study. A reference SCC composition was designed using cement type CEM I 42.5 R (supplied by Cementos Portland Valderrivas and designated according to European standard EN 196–1), limestone filler Betocarb® P1-DA (85 ± 5% under 63 µm, supplied by Omya Clariana SA), a polycarboxylate ether based high range water reducing admixture (HRWRA, supplied by Master Builders Solutions SLU) and natural siliceous aggregates, 0–4 sand and 4–20 coarse aggregate. The reference mixture was modified incorporating combinations of NC and VMAs, according to the enhanced performance of SCC pastes rheological parameters (structural build-up) evaluated in a previous study [23]. The amount of HRWRA was adjusted in each mixture to achieve a 650 ± 10 mm of spread diameter.

Three types of viscosity modifying admixture (VMA) were used:

- A poly (acrylamide-co-acrylate)-based viscosity modifying admixture (VMA1).
- A polyether-methylcellulose-based viscosity-modifying admixture (VMA2).
- A synthetic co-polymer viscosity-modifying admixture (VMA3).

All VMAs were used at 0.2 % by cement weight, and VMA2 was also used at 0.4 %.

A 2 % by cement weight of five types of nanocomponents (NC) were also incorporated:

- Attapulgite nanoclay (palygorskite) (ATT), with needle shaped particles of D (4,3) – De Brouckere Mean Diameter – of 21.97 µm and a BET surface of 144 m^2/g.
- Bentonite nanoclay (montmorillonite) (BE) with plate shaped particles of D (4,3) of 38.42 µm and a BET surface of 138 m^2/g.
- Two types of sepiolite nanoclays (palygorskite) with needle shaped particles, one in a powder form (SEP), with a D (4,3) of 39.66 µm and a BET surface of 316 m^2/g, and other dispersed in water (SEW), with a D (4,3) of 57.7 µm and a BET surface of 284 m^2/g.
- A water-based colloidal nanosilica (NS), MasterRoc MS 685 supplied by Master Builders Solutions España, SLU, with a density of 1.134 g/cm^3 and 22 % of solid content.

2.2. Experimental methods

2.2.1. Lateral pressure column setups: self-weight and air pressure

Fig. 1 sketches the laboratory experimental setup used in this study to measure the lateral pressure exerted by the SCC fresh samples after poured inside a mold. The basic component of the testing setups consisted in a cylindrical steel mold of 500 mm of height and 160 mm of diameter with lateral openings at different heights available for inserting thermocouples (Ti), wall pressure transmitters (P_W) and capillary pressure sensors (P_C). Two molds were attached together, one on the other, reaching a 1 m height column, procuring a self-weight pressure column test (SWP). In addition, the top of the mold was adapted to allow air pressurization of SCC samples. Pressure was adjusted with a pressure regulator connected to an air compressor, obtaining an air pressure column test (APC). In both cases, columns were filled with SCC samples leaving a 5 cm gap at the top.

2.2.2. Temperature and capillary and wall pressure devices

Temperature (T) and lateral (P_W) and capillary (P_C) pressure were recorded during the test. Thermocouples were embedded inside the SCC samples for temperature measure. Wall pressure transmitters model WIKA s-11 (0–160 kPa) were placed directly on the SCC sample, attached to the steel mold, and aligned with the internal side. Each capillary pressure sensor Sensortechnics RVA (0–250 kPa) was connected to a plastic pipe filled with water which was inserted to the SCC samples after casting, pierced through holes drilled on the mold covered with tape to avoid leakages.

Fig. 2 plots the experimental results obtained in the SWC and APC tests of temperature (T – dotted lines) and lateral pressure measured with wall (P_W – continuous lines) and capillary (P_C – dashed lines) pressure sensors over time on reference SCC samples. All measurements were related to the moment when mixing began. It can be observed that pressure was measured after 15–20 min after mixing on SWC test, when the mold was filled with SCC, while the first measurements on APC delayed 40 min to be achieved.

Temperature showed an increase after SCC was introduced in the mold, followed by a dormant period, an increase at around 2–4 h, reaching the maximum value at 12–14 h, and finally a soft decay. This thermal profile is typical for cement-based materials during setting.

Regarding pressure values, SWC showed an initial zero value until SCC sample was casted in the mold. A maximum pressure value was

Table 1
SCC compositions (components in kg).

Mixture	CEM I 42.5 R	Limestone filler	Sand	Coarse aggr.	Water	HRWRA (%)	VMA (%)	Nanoclay (%)
REF	350	175	442	597	183	0.6	–	–
VMA2BE	350	175	442	597	183	0.6	0.2	2
VMA2(0.4)BE	350	175	442	597	183	0.8	0.4	2
VMA2AT	350	175	442	597	183	0.6	0.2	2
VMA3NS	350	175	442	597	151[*a]	1.4	0.2	2
VMA1SEP	350	175	442	597	183	2	0.2	2
SEW	350	175	442	597	151[*a]	1	–	2

*a Water of the liquid components (SEW and NS) was also considered. SEW and NS solid residue is 22%.

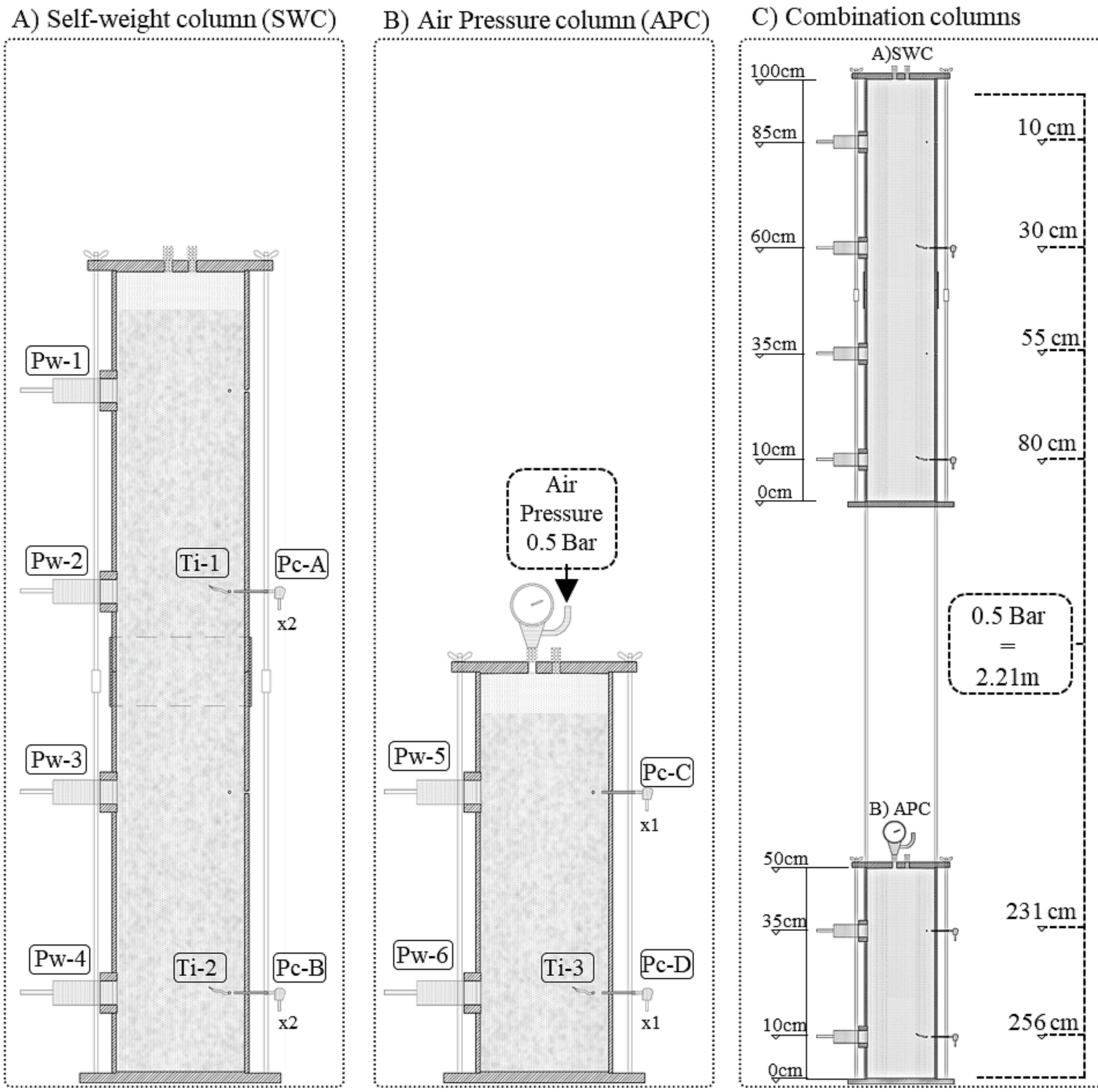

Fig. 1. Lateral pressure experimental setups: self-weight pressure column test and air pressure column test.

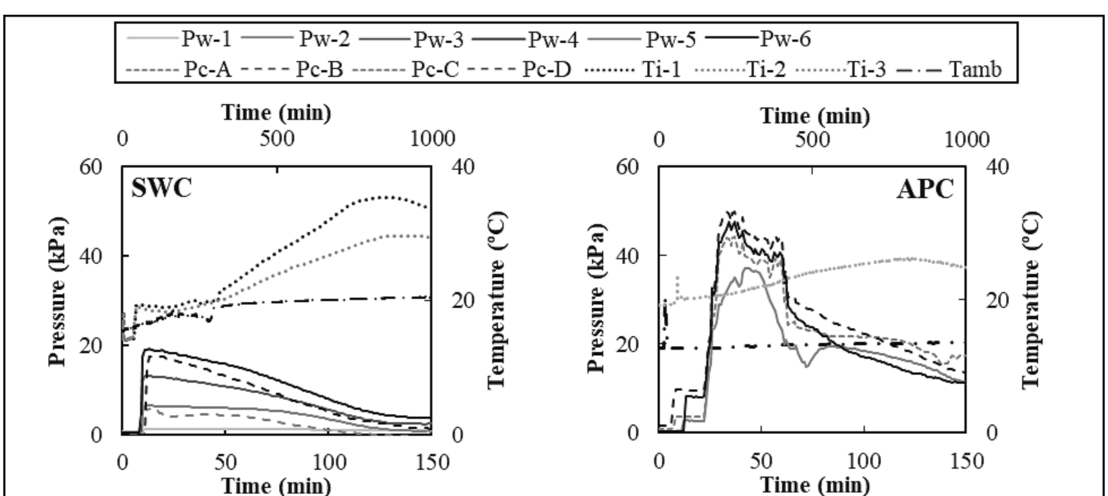

Fig. 2. Internal Temperature (Ti) and Lateral pressure measured with wall (Pw) and capillary (Pc) pressure sensors over time on reference SCC measured in the self-weight pressure column test (SWC) and the air pressure column test (APC).

followed by a smooth pressure decrease that was stabilized after 120 min. In the APC, pressure increased when the sample was casted and air pressure was injected in the mold until reaching the target pressure of 0.5 bar (50 kPa), followed again by a pressure decrease. It can be observed that P_W and P_C values showed the same pattern on both tests, although slight differences of the pressure values were recorded.

However, pressure values obtained after 120 min showed measurement problems as: Some wall pressure transmitters recorded an increase of pressure instead of expected decay. That effect is due to tension stresses produced by shrinkage of the SCC stuck to the sensor. In contrast, capillary pressure sensors registered negative values produced by water suction in the system as the amount of water available is reduced due to cement hydration. Accordingly, pressure measurements on fresh SCC samples were considered up to 120 min.

The experimental results obtained from the SWC and the APC tests of the same SCC mixture could therefore be combined as depicted in Fig. 1, considering the column height equivalent to the air pressure applied (air pressure = 0.5 bar), estimating SCC density as 2.5 g/cm^3. This combination allowed evaluating in laboratory conditions and with small size samples casting depths up to 2.66 m, recording P_W measurements at 0.10, 0.30, 0.55, 0.80, 2.31 and 2.56 m and P_C measurements at 0.30, 0.80, 2.31 and 2.56 m of depth.

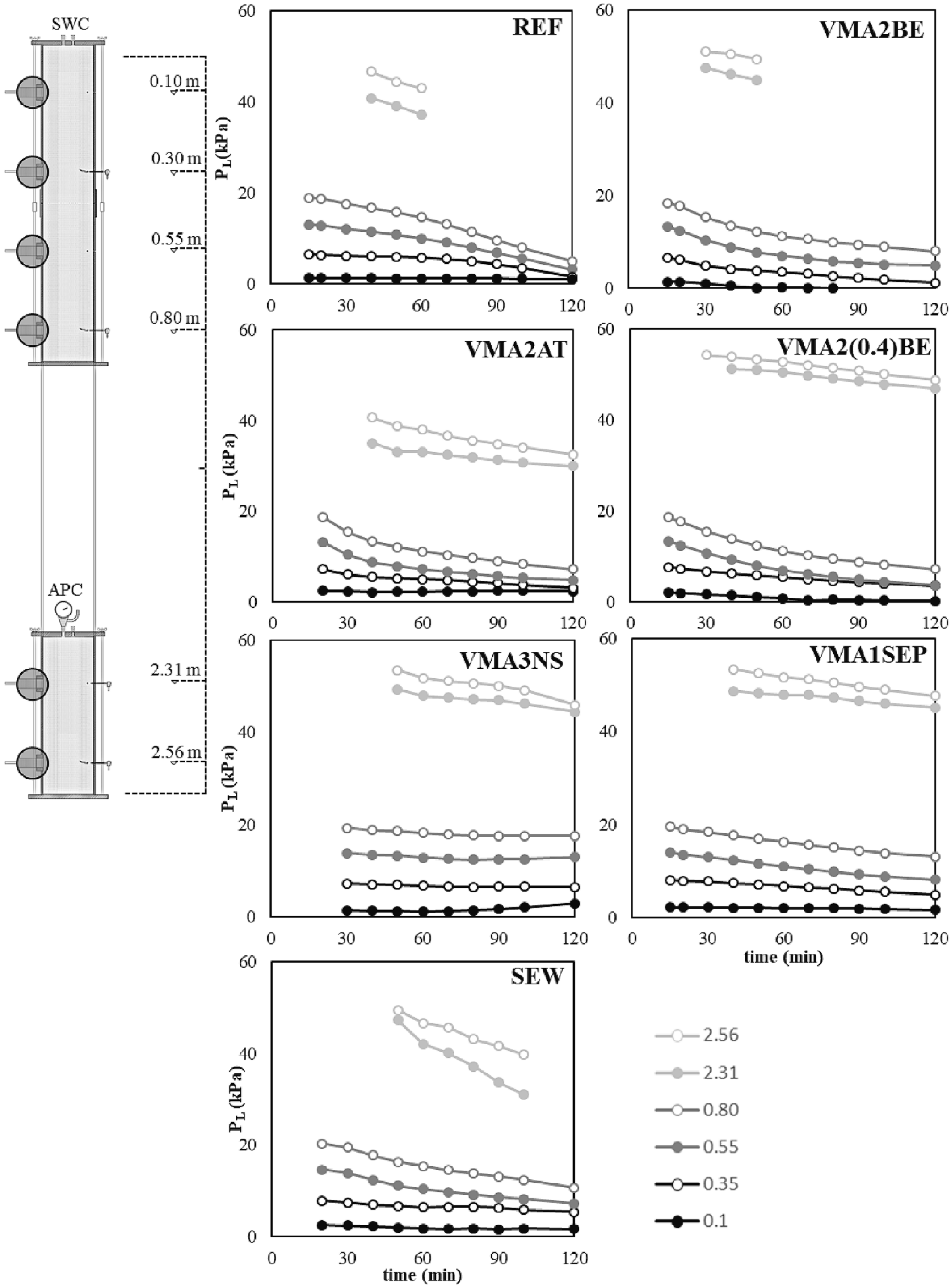

Fig. 3. Wall lateral pressure over time in the combined column experimental setup.

3. Experimental results

Wall lateral pressure measurements (P_W) over time in the combined column experimental setup are plotted in Fig. 3. Measurements were recorded for SWC from 15 min, while APC took longer to get readings, due to the time needed to put the sample under air pressure (Fig. 2), and the first measurements were logged 40–50 min after mixing began. Some APC measurements were incomplete due to difficulties to maintain a constant air pressure on the samples during the tests.

It was observed that the incorporation of NC reduced the initial pressure in some mixtures (AT and BE) for which the amount of HRWRA remained low, while NS, SEP and SEW samples, which required larger amounts of HRWRA, slightly increased P_W. This reduction was larger in SWC than in APC tests. However, the most important change observed was the fastest pressure decay from 15 to 60 min produced by all NC but NS, regarding the reference SCC (REF). The fastest decrease was measured for AT, followed by BE, SEW and SEP, respectively. Regarding the amount of VMA2 in samples with BE, larger amount of VMA (0.4) accelerated P_W reduction.

Capillary lateral pressure (P_C) measurements in the combined column experimental setup over time are presented in Fig. 4. Four capillary pressure devices were used at four different column heights. It can be

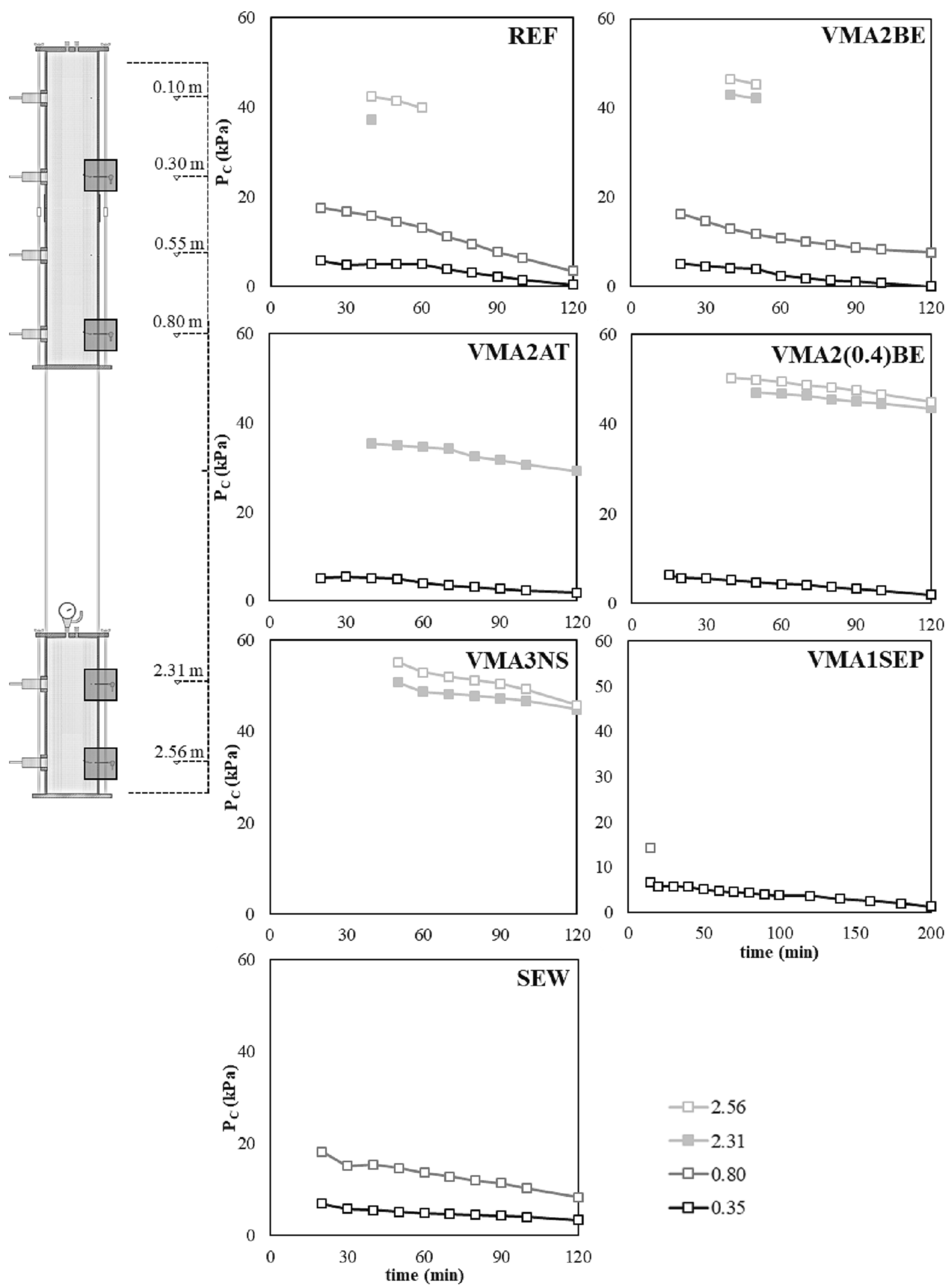

Fig. 4. Capillary lateral pressure over time in the combined column experimental setup.

observed that some measurements were not recorded due to the failure of some devices, because any loss of water from the pipe connecting the pressure device to the SCC sample introduced air bubbles that hindered sensor operation. Therefore, this set of P_C results did not allow reaching partial conclusions by themselves. Nevertheless, the valid experimental measurements of capillary pressure sensors correlated quite well with those obtained with wall pressure transmitters.

Table 2 presents the maximum lateral pressure values (P_{max}) measured on SWC and APC experimental setups with wall and capillary pressure sensors at different depths (H in meters) and the ratio between P_{max} and depth (H) for each SCC composition. In order to present a complete set of values measured simultaneously, a reference time of 40 min after mixing was selected, which could be a good approximation to the time necessary to fill a formwork for a real scale structural member [12].

4. Analysis and discussion

4.1. Wall pressure vs. Capillary pressure measurements

Fig. 5 relates lateral pressure measured with wall (P_W) and capillary (P_C) pressure sensors at different depths and on different SCC compositions. Both types of devices measured similar pressure values independently of measure depth or SCC composition, as described elsewhere [15]. Consequently, two conclusions can be reached. First, both types of pressure sensing devices can be used to evaluate lateral pressure, although is easier and more reliable to use wall than capillary pressure sensors. And second, lateral pressure exerted by SCC suspensions on the formwork wall was mainly due to the pressure produced in the liquid phase, which is the same on the wall surface and inside the suspension. Accordingly, the wall effect that could be expected due to friction of SCC against the formwork [6] can be neglected, independently of the depth of measurement.

4.2. Self-weight column vs. Air column on lateral pressure measurements

When the experimental results obtained with SWC and APC setups are plotted together (Figs. 3 and 4), considering the equivalent sample height produced by air pressure, a good correlation between lateral pressure and height was observed. Therefore, APC can be considered an advantageous option for experimental purposes in the laboratory, as different pressure conditions, equivalent to different column heights, can be tested with smaller samples and fewer pressure sensors.

However, some issues could arise due to the difficulties to maintain the air pressure on the sample without leaks of material or air. Besides, it is not clear if the lack of fresh material on the upper part of the tested sample could facilitate the migration of water (bleeding) from the lower part of the sample, modifying the pressure readings over time due to earlier consolidation related to lower water to cement ratio [13]. As a third point, the temperature of the SCC sample during the test was lower in the APC than the SWC, it took longer to record the first pressure measurement and the pressure readings were less stable, as can be observed in Fig. 2. Finally, this reduced size column could be affected by the side effects of sample proportions (height regarding width) and the local effects due to the proximity to the sample bottom [6], which can limit the relevance of the laboratory results for real scale applications.

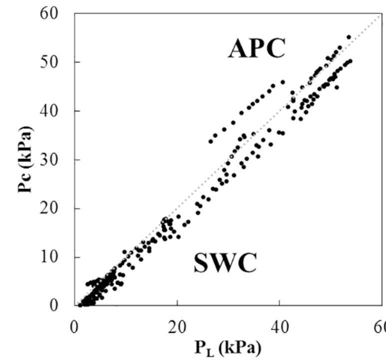

Fig. 5. Lateral pressure measured with wall (Pw) and capillary (Pc) pressure sensors at different depths and on different SCC compositions.

4.3. Effect of combined NC and VMA on maximum lateral pressure (P_{max})

The experimental results of P_W measured in SWC and APC pressure tests can be combined to evaluate the effect of column height (H) on P_W. Fig. 6 plots the linear adjustment of the maximum lateral pressure values (P_{max} in kPa) listed in Table 2 and column height (H in cm) for the combination of experimental results measured with wall pressure transmitters. Each SCC mixture results were adjusted, and a P_{max}/H mixture coefficient was obtained.

According to the literature [4,5], P_{max}/H should be related to the rheological properties of the paste phase of the SCC samples. Table 3 presents the experimentally measured values of the SCC paste thixotropy coefficient ($A_{thix,p}$) measured with DSR and a Controlled Stress protocol (CS) from 10 to 60 min [23]. Fig. 7 shows yield stress values (τ_0) over time obtained from CS. These values were used to calculate $A_{thix,p}$ according to Eq.1 [16], where τ_t was the yield stress at time t (in min) and τ_0 was the initial yield stress (in Pa),

$$\tau_t = \tau_0 + A_{thix} t \quad (1)$$

Fig. 8 relates P_{max}/H values obtained in Fig. 6 and $A_{thix,p}$ presented in Table 3. A good linear correlation was obtained for all NE-SCC samples except AT. This fact could be related to wrong rheology measurements of the NE-SCC paste, due to AT particle migration on DSR tests applied over time to the same sample [20], or to an unexpected performance of SCC with AT, due to the adsorption of part of the HRWRA by the finer

Table 2
Initial Maximum lateral pressure (P_{max}) evaluated on Self-weight pressure column (SWC) and air pressure column (APC), measured with wall and capillary devices at 40 min after mixing began.

	Wall lateral pressure (kPa)						Capillary pressure (kPa)				
	SWC				APC		SWC		APC		
Depth (m)	Pw-1 (0.1)	Pw-2 (0.3)	Pw-3 (0.55)	Pw-4 (0.8)	Pw-5 (2.31)	Pw-6 (2.56)	Pc-A (0.3)	Pc-B (0.8)	Pc-C (2.31)	Pc-D (2.56)	P_{max}/H
REF	1.3	6.1	11.3	16.5	40.03	45.53	5.8	17.5	37.1	42.3	18
VMA2BE	1.4	4.1	8.5	13.2	45.84	49.3	5.1	16.3	43.0	46.5	19
VMA2(0.4) BE	2.2	6.14	8.95	13.50	51.74	53.81	6.4	–	44.8	50.2	21
VMA2AT	1.9	5.27	8.5	13	35.02	40.64	5.2	–	35.3	45.8	15
VMA3NS	2.4	7.08	13.48	18.85	50.04	53.82	6.0	15.7	50.8	55.1	21
VMA1SEP	1.4	7.33	12.16	17.53	54.06	58.67	6,7	14.3	–	–	23
SEW	2.5	6.97	12.16	17.43	47.15	49.66	7.0	18.2	–	–	20

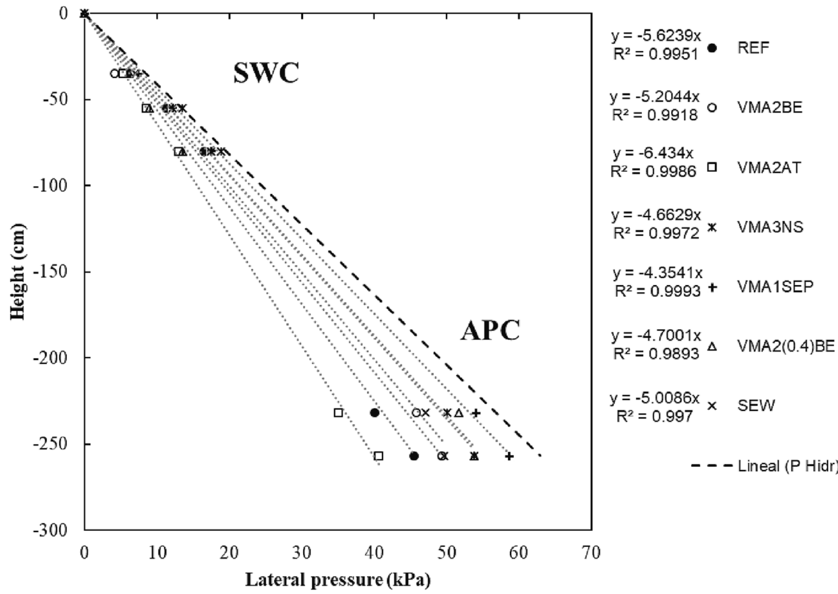

Fig. 6. Maximum lateral pressure (P_{max}) at different depths of NE-SCC samples (results combining data measured in self-weight and air pressure columns).

Table 3
Thixotropy coefficient of the paste ($A_{thix,p}$) measured with DSR and a Stress Controlled protocol from 10 to 60 min and pressure decay coefficient (C_d) of SCC compositions.

SCC composition	$A_{thix,p}$ (Pa/min)	C_d (kPa/m·h)
REF	–	9.02
VMA2BE	2.9	7.32
VMA2(0.4)BE	1.45	5.22
VMA2AT	4.7 (*)	4.5
VMA3NS	1.49	2.06
VMA1SEP	0.74	4.04
SEW	2.08	6.37

* Calculated according to Eq. (3).

particles of the aggregate [36]. The amount of HRWRA of the SCC paste with AT was the lowest of the set, jointly with BE, althouth they did not follow the same pattern. In this case, the plate shape of BE particles would make more difficult HRWRA adsorption by the finer aggregate particles and, consequently, mixtures with AT would be more affected by the effects of HRWRA absorption than BE.

According to the linear adjustment obtained in Fig. 8, P_{max} exerted by NE-SCC at 40 min can be expressed empirically as a function of the paste thixotropy coefficient ($A_{thix,p}$ in Pa/min), measured with DSR and a Stress Controlled protocol from 10 to 60 min [23], and the height of the SCC element (H in m) as per Eq. (2):

$$P_{max} = \left(24 - 1.8A_{thix,p}\right)H \tag{2}$$

Eq. (2) is in good agreement with the model by Ovarlez and Roussel [6], considering P_{max} as the difference between the hydrostatic pressure (P_H) and the reduction of pressure produced by the increase of yield stress in time, equivalent to $A_{thix,p}$, influenced by the height (H). Eq. (2) can also be expressed as per Eq. (3).

$$P_{max} = P_H - KA_{thix,p}H \tag{3}$$

Relating Eq. (2) with Eq.3, 24H (kPa) seems in good agreement with P_H, as per Eq. (4),

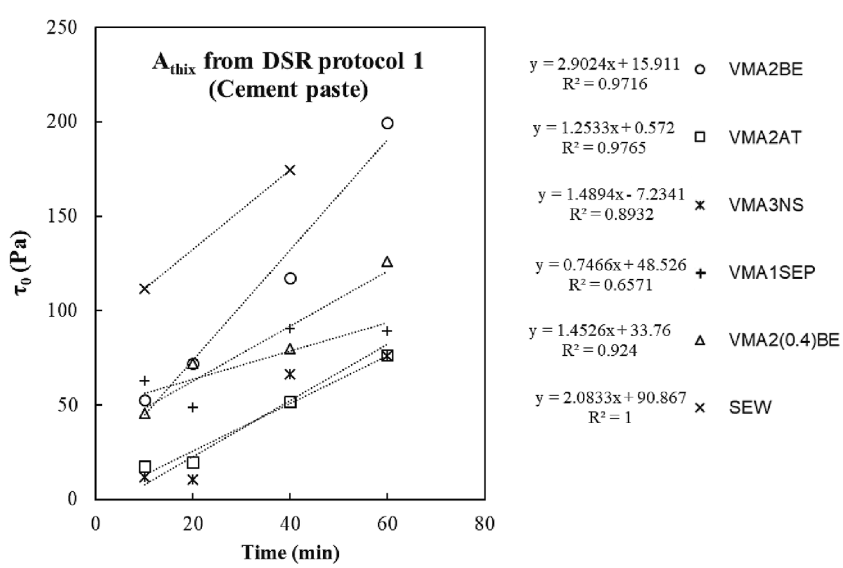

Fig. 7. Shear yield stress over time measured with controlled stress protocol (CS) on DSR and calculated $A_{thix,p}$.

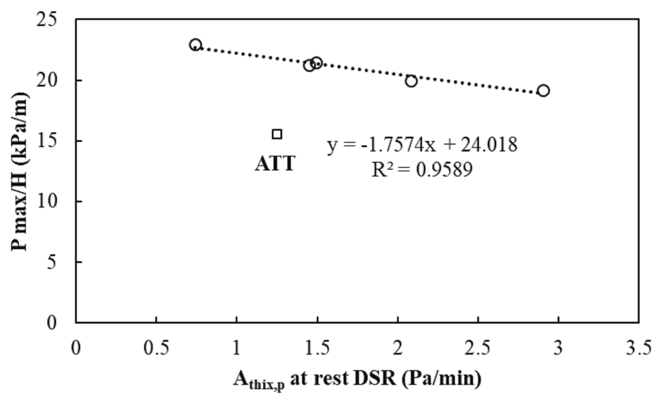

Fig. 8. Maximum initial pressure Pmax (in kPa) exerted by SCC samples by depth (in cm) related to the thixotropic coefficient (Athix) of the correspondent SCC paste measured with DSR CS [Varela 2021].

$$P_H(kPa) = \rho g H = 2.5\ (\mathrm{g/cm^3}) * 9.8\ (\mathrm{m/s^2}) * H(\mathrm{m}) = 24.5\ H(\mathrm{kPa}) \quad (4)$$

K is in this case a constant (1.8, when H is in m and $A_{thix,p}$ in Pa/min) and would be probably affected by the ratio of aggregate and paste of the reference SCC [20,36], the casting rate and the mold section [6]. Accordingly, AT mixture could be adjusted to Eq. (2) and its effective $A_{thix,p}$ would be 4.7 Pa/min.

4.4. Effect of combined NC and VMA on lateral pressure evolution over time (P_L)

As shown in Fig. 3, the lateral pressure (P_L) exerted on the mold by SCC decays over time. The evolution of P_L can be calculated as the difference between P_{max} and the reduction of lateral pressure over time (ΔP), as expressed in Eq. (5).

$$P_L = P_{max} - \Delta P \quad (5)$$

Eq. (6) is proposed to calculate ΔP,

$$\Delta P = C_d \cdot H \cdot t \quad (6)$$

where H is the height of the structural member (in m), t is the time elapsed since reaching the maximum value P_{max} (in h) and C_d is an empirical SCC pressure decay coefficient (in kPa/m·h) calculated as the average P_L decay measured for each NE-SCC composition evaluated in this study. C_d values calculated for the experimental data recorded in this study are listed in Table 3.

Replacing the value of P_{max} of Eq. (3) in Eq. (6), a predictive analytical model, combining physical and empirical parameters is presented in Eq. (7),

$$P_L = P_H - KA_{thix,p}H - C_d \cdot H \cdot t = (\rho g - KA_{thix,p} - C_d \cdot t) \cdot H \quad (7)$$

Fig. 9 relates the measured and calculated values of NE-SCC lateral pressure, according to Eq. (7). A good correlation can be observed for both SWC (0–20 kPa) and APC (30–60 kPa) experimental results for all NE-SCC mixtures.

The overall lateral pressure exerted on the mould by the NE-SCC, considering the initial filling time, can be modelled as depicted in Fig. 10. The maximum lateral pressure occurred 40 min after the initial mixing time and was the hydrostatic pressure less the initial effect of A_{thix}. P_L decayed according to a decay coefficient C_d, which could not be linked to A_{thix}, probably because the cement hydration processes already were fully activated.

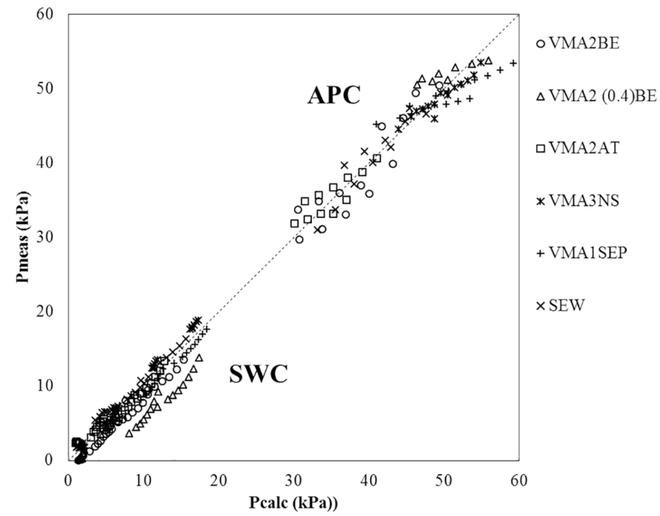

Fig. 9. Lateral pressure (P_L) of NE-SCC measured and calculated according to Eq. (7).

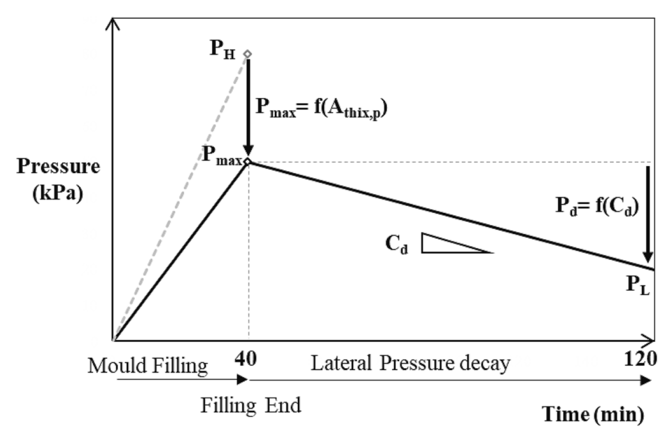

Fig. 10. Lateral pressure (P_L) exerted by NE-SCC on the mold over time, considering the time required to fill-in the mold.

5. Conclusions

An experimental study on the combined effect of nanosilica (NS), four types of nanoclays (NC): Attapulgite (AT), Bentonite (BE) and Sepiolite in powder form (SEP) and dispersed in water (SEW), and three types of viscosity modifier admixtures (VMA) on the lateral pressure exerted on the formwork by nano engineered self-compacting concretes (NE-SCC) was presented. An experimental setup which combined a self-weight column (SWC) of 1 m and an air pressure column tests (APC) of 0.5 m, both instrumented with thermocouples (T), wall pressure transmitters (P_W) and capillary pressure sensors (P_C), was used to evaluate the material and correlate wall and air pressure results.

A predictive model of the maximum Lateral pressure value (P_{max}) and its evolution over time (P_L) considering the hydrostatic pressure (P_H), the thixotropy coefficient of the SCC paste ($A_{thix,p}$) and the structuration rate coefficient of SCC (C_d) was proposed. This model partially follows the existing physical and empirical models that can be found in the literature.

The main findings of the study were:

- Wall pressure transmitters showed to be more reliable than the capillary pressure sensors used in this study, although both were able to measure similar pressure values. Accordingly, it was concluded that P_L depends mainly on pressure exerted by the liquid phase of SCC mixtures and that friction of SCC against the mold can be considered negligible for these mixtures.

- APC is a very cheap and versatile laboratory test setup that can produce pressure results for different simulated member heights with a small sample and few pressure sensors. However, the risk of air or material leakages makes SWC test easier to use than APC.
- P_{max} exerted by SCC can be related to the structural build-up capacity (thixotropy) of fresh SCC paste measured with $A_{thix,p}$. Accordingly, designing SCC pastes with enhanced $A_{thix,p}$ can be considered an effective way to reduce P_{max} exerted by SCC. In one case (AT), the evaluation of SCC paste samples with DSR CS protocol underestimated NC efficiency.
- The combination of NC and VMAs reduced P_{max} of SCC in an efficient way, considering the low amount of material required. Particularly, combined BE and AT with VMA2 samples showed a high reduction of P_{max} during the first hour. The larger the amount of VMA2, the larger the reduction.
- The evolution of P_L during the first hour after mixing depended mainly on $A_{thix,p}$. Afterwards, form 60–120 min, P_L decreased according to SCC structuration rate over time, which can be evaluated with the empirical pressure decay coefficient (C_d). A relation between $A_{thix,p}$ and C_d could not be found.

CRediT authorship contribution statement

Hugo Varela: Conceptualization, Methodology, Formal analysis, Investigation, Writing – original draft, Visualization. **Gonzalo Barluenga:** Conceptualization, Methodology, Investigation, Resources, Writing – original draft, Project administration, Funding acquisition. **Javier Puentes:** Conceptualization, Methodology, Investigation, Writing – review & editing. **Irene Palomar:** Conceptualization, Methodology, Investigation, Writing – review & editing. **Angel Rodriguez:** Conceptualization, Methodology, Validation, Investigation, Writing – review & editing.

Declaration of Competing Interest

The authors declare that they have no known competing financial interests or personal relationships that could have appeared to influence the work reported in this paper.

Data availability

Data will be made available on request.

Acknowledgements

The authors acknowledge with thanks the financial support provided by the projects NanoCompaC (BIA2016-77911-R), funded by the Spanish Ministry of Economy and Competitiveness, and Print3Dcement (PID2019-106525RB-I00), funded by the Spanish Ministry of Science and Innovation, and the Grant for training of Lecturers (FPU-UAH 2019), funded by University of Alcalá. Finally yet importantly, the authors are grateful to TOLSA GROUP S.A, Master Builders Solutions España SLU, Omya Clariana and Cementos Portland Valderrivas, SA for supplying at no charge some components used in the tests.

References

[1] N. Gowripalan, P. Shakor, P. Rocker, Pressure exerted on formwork by self-compacting concrete at early ages: A review, Case Stud. Constr. Mater. 15 (2021) e00642.

[2] T. Proske, K.H. Khayat, A. Omran, O. Leitzbach, Form pressure generated by fresh concrete: a review about practice in formwork design, Mater. Struct. 47 (7) (2014) 1099–1113.

[3] J. Assaad, K.H. Khayat, H. Mesbah, Variation of formwork pressure with thixotropy of self-consolidating concrete, ACI Mater. J. 100 (1) (2003) 29–37, https://doi.org/10.14359/12460.

[4] J. Assaad, K.H. Khayat, Kinetics of formwork pressure drop of self-consolidating concrete containing various types and contents of binder, Cem. Concr. Res. 35 (8) (2005) 1522–1530, https://doi.org/10.1016/j.cemconres.2004.12.005.

[5] J. Assaad, K. Khayat, Formwork Pressure of Self-Consolidating Concrete Made with Various Binder Types and Contents, ACI Mater. J. 102 (4) (2005) 215–223, https://doi.org/10.14359/14613.

[6] G. Ovarlez, N. Roussel, A physical model for the prediction of lateral stress exerted by self-compacting concrete on formwork, Mater. Struct. 39 (2006) 269–279, https://doi.org/10.1617/s11527-005-9052-1.

[7] J.H. Kim, M. Beacraft, S.P. Shah, Effect of mineral admixtures on formwork pressure of self-consolidating concrete, Cem. Concr. Compos. 32 (2010) 665–671, https://doi.org/10.1016/j.cemconcomp.2010.07.018.

[8] S.H. Kwon, S.P. Shah, Q.T. Phung, J.H. Kim, Y. Lee, Intrinsic Model to Predict Formwork Pressure, ACI Mater. J. 107 (1) (2010) 20–26, https://doi.org/10.14359/51663460.

[9] K.H. Khayat, A.F. Omran, Field Validation of SCC Formwork Pressure Prediction Models, Concr. Int. 33 (6) (2011) 33–39.

[10] N.J. Gardner, L. Keller, R. Quattrociocchi, G. Charitou, Field investigation of formwork pressures using self-consolidating concrete, Concr Int 34 (1) (2012) 41–47.

[11] A. Perrot, A. Pierre, S. Vitaloni, V. Picandet, Prediction of lateral form pressure exerted by concrete at low casting rates, Mater. Struct. 48 (2015) 2315–2322, https://doi.org/10.1617/s11527-014-0313-8.

[12] P. Billberg, N. Roussel, S. Amziane, M. Beitzel, G. Charitou, B. Freund, J. N. Gardner, G. Grampeix, C.A. Graubner, L. Keller, K.H. Khayat, D.A. Lange, A. F. Omran, A. Perrot, T. Proske, R. Quattrociocchi, Y. Vanhove, Field validation of models for predicting lateral form pressure exerted by SCC, Cem. Concr. Compos. 54 (2014) 70–79, https://doi.org/10.1016/j.cemconcomp.2014.02.003.

[13] M. Tuyan, R.S. Ahari, T.K. Erdem, Ö.A. Çakır, K. Ramyar, Influence of thixotropy determined by different test methods on formwork pressure of self-consolidating concrete, Construction and Building Materials 173 (2018) 189–200, https://doi.org/10.1016/j.conbuildmat.2018.04.046.

[14] P. Ghoddousi, A.A. Shirzadi Javid, G. Ghodrati Amiri, K. Donyadideh, Predicting the formwork lateral pressure of self-consolidating concrete based on experimental thixotropy values, Int. J. Civ. Eng. 17 (7) (2019) 1131–1144, https://doi.org/10.1007/s40999-018-0368-y.

[15] K.H. Khayat, J.J. Assaad, Measurement systems for determining formwork pressure of highly-flowable concrete, Mater. Struct. 41 (2008) 37–46, https://doi.org/10.1617/s11527-006-9216-7.

[16] N. Roussel, A thixotropy model for fresh fluid concretes: Theory, validation and applications, Cem. Concr. Res. 36 (2006) 1797–1806, https://doi.org/10.1016/j.cemconres.2006.05.025.

[17] N. Roussel, G. Ovarlez, S. Garrault, C. Brumaud, The origins of thixotropy of fresh cement pastes, Cem. Concr. Res. 42 (2012) 148–157, https://doi.org/10.1016/j.cemconres.2011.09.004.

[18] R. Ferron, A. Gregori, Z. Sun, S.P. Shah, Rheological Method to Evaluate Structural Build-Up in Self-Consolidating Concrete Cement Paste, ACI Mater. J. 104:3 (2007) 242-250. doi: 10.14359-18669.

[19] T. Lecompte, A. Perrot, Non-linear modeling of yield stress increase due to SCC structural build-up at rest, Cem. Concr. Res. 92 (2017) 92–97, https://doi.org/10.1016/j.cemconres.2016.11.020.

[20] F. Mahaut, S. Mokéddem, X. Chateau, N. Roussel, G. Ovarlez, Effect of coarse particle volume fraction on the yield stress and thixotropy of cementitious materials, Cem. Concr. Res. 38 (11) (2008) 1276–1285, https://doi.org/10.1016/j.cemconres.2008.06.001.

[21] N. Roussel, H. Bessaies-Bey, S. Kawashima, D. Marchon, K. Vasilic, R. Wolfs, Recent advances on yield stress and elasticity of fresh cement-based materials, Cem. Concr. Res. 124 (2019), 105798, https://doi.org/10.1016/j.cemconres.2019.105798.

[22] G. Barluenga, I. Palomar, C. Guardia, H. Varela, F. Hernandez-Olivares, Rheology and Build-Up of Fresh SCC Pastes Evaluated with the Mini-slump Cone Test. In: V. Mechtcherine, K. Khayat, E. Secrieru (eds.), Rheology and Processing of Construction Materials. RheoCon 2019, SCC 2019. RILEM Bookseries, Springer, 2020, pp. 160-167. doi: 10.1007/978-3-030-22566-7_19.

[23] H. Varela, G. Barluenga, I. Palomar, A. Sepulcre, Synergies on rheology and structural build-up of fresh cement pastes with nanoclays, nanosilica and viscosity modifying admixtures, Constr. Build. Mater. 308 (2021), 125097, https://doi.org/10.1016/j.conbuildmat.2021.125097.

[24] S. Kawashima, P. Hou, D.J. Corr, S.P. Shah, Modification of cement-based materials with nanoparticles, Cem. Concr. Compos. 36 (2013) 8–15, https://doi.org/10.1016/j.cemconcomp.2012.06.012.

[25] S. Kawashima, M. Chaouche, D.J. Corr, S.P. Shah, Rate of thixotropic rebuilding of cement pastes modified with highly purified attapulgite clays, Cem. Concr. Res. 53 (2013) 112–118, https://doi.org/10.1016/j.cemconres.2013.05.019.

[26] L. Senff, J.A. Labrincha, V.M. Ferreira, D. Hotza, W.L. Repette, Effect of nano-silica on rheology and fresh properties of cement pastes and mortars, Constr. Build. Mater. 23 (2009) 2487–2491, https://doi.org/10.1016/j.conbuildmat.2009.02.005.

[27] P.K. Hou, S. Kawashima, K.J. Wang, D.J. Corr, J.S. Qian, S.P. Shah, Effects of colloidal nanosilica on rheological and mechanical properties of fly ash–cement mortar, Cem. Concr. Compos. 35 (2013) 12–22, https://doi.org/10.1016/j.cemconcomp.2012.08.027.

[28] A. Kaci, M. Chaouche, P.-A. Andréani, Influence of bentonite clay on the rheological behaviour of fresh mortars, Cem. Concr. Res. 41 (2011) 373–379, https://doi.org/10.1016/j.cemconres.2011.01.002.

[29] H. Varela, G. Barluenga, I. Palomar, Influence of nanoclays on flowability and rheology of SCC pastes, Constr. Build. Mater. 243 (2020), 118285, https://doi.org/10.1016/j.conbuildmat.2020.118285.
[30] K. Kawashima, K. Wang, R.D. Ferron, J.H. Kim, N. Tregger, S. Shah, A review of the effect of nanoclays on the fresh and hardened properties of cement-based materials, Cem. Concr. Res. 147 (2021), 106502, https://doi.org/10.1016/j.cemconres.2021.106502.
[31] S. Ma, S. Kawashima, Investigating the Working Mechanisms of Viscosity-Modifying Admixtures through Rheological and Water Transport Properties, J. Mater. Civ. Eng. 32 (2020) 04019357, https://doi.org/10.1061/(ASCE)MT.1943-5533.0003018.
[32] D. Bülichen, J. Kainz, J. Plank, Working mechanism of methyl hydroxyethyl cellulose (MHEC) as water retention agent, Cem. Concr. Res. 42 (2012) 953–959, https://doi.org/10.1016/j.cemconres.2012.03.016.
[33] M. Palacios, R.J. Flatt, Working mechanism of viscosity-modifying admixtures, In: P-C. Aïtcin, R. J. Flatt (eds.), Science and Technology of Concrete Admixtures, Woodhead Publishing, Elsevier, 2016, pp. 415-432. doi: 10.1016/B978-0-08-100693-1.00020-5.
[34] I. Palomar, G. Barluenga, C. Guardia, M.C. Alonso, M. Álvarez, Rheological Characterization of Self-compacting Concrete Pastes with Polymeric Admixtures. In: V. Mechtcherine, K. Khayat, E. Secrieru (eds.), Rheology and Processing of Construction Materials. RheoCon 2019, SCC 2019. RILEM Bookseries, Springer, 2020, pp.491-499. doi: 10.1007/978-3-030-22566-7_57.
[35] Y. Qian, G. De Schutter, Enhancing thixotropy of fresh cement pastes with nanoclay in presence of polycarboxylate ether superplasticizer (PCE), Cem. Concr. Res. 111 (2018) 15–22, https://doi.org/10.1016/j.cemconres.2018.06.013.
[36] J. Yammine, M. Chaouche, M. Guerinet, M. Moranville, N. Roussel, From ordinary rhelogy concrete to self compacting concrete: A transition between frictional and hydrodynamic interactions, Cem. Concr. Res. 38 (7) (2008) 890–896, https://doi.org/10.1016/j.cemconres.2008.03.011.